Rates of Electron-Impact Transitions between Excited States of Helium

L. C. Johnson and E. Hinnov
Plasma Physics Laboratory, Princeton University, Princeton, New Jersey 08540
(Received 24 June, 1969)

Measurements of electron densities and population densities of excited states of neutral helium are presented for afterglows in the C stellarator. Electron densities range from 10^{11} to 3×10^{13} cm^{-3}, and electron temperatures range from 0.04 to 1 eV. Semiempirical cross-section formulas for transitions among excited levels are deduced by comparing observed excited-state population densities with solutions of detailed transition-rate equations. The agreement between computed and measured values is good, when the assumed cross sections are comparable with impact-parameter approximation results; the agreement is poor — especially at low electron densities and temperatures — when classical cross sections are assumed.

I. INTRODUCTION

The rate of transitions of atoms between their various excited states by means of electron collisions is one of the major considerations in the analysis of excitation and ionization processes in plasmas. The cross sections for such transitions cannot be measured directly, as can those for transitions from the ground state, so that one must rely upon approximate theoretical cross sections or deductions from indirect measurements.

The cross sections most commonly used[1] are the classical impulse-approximation cross sections of Gryziński,[2,3] a notable application being the studies of recombining plasma by Bates, Kingston, and McWhirter.[4] The reason for using the classical cross sections is that they provide a relatively simple set of functions that seem to reproduce experimental observations with tolerable accuracy,[2,3,5–10] even though there are considerable misgivings about the universal applicability of these cross sections.[11–13]

A different set of cross sections is provided by the impact-parameter approximation of Seaton.[14] The transitions of greatest significance in excitation problems are those in which the principal quantum number changes by unity ($n \rightleftarrows n+1$) and also, in nonhydrogenic atoms, those in which n does not change. For such transitions the impact-parameter cross sections are not very different from Gryziński's classical cross sections for small n, but the differences grow fairly rapidly with increasing n; the Gryziński cross sections being the larger near the threshold energies.

A review of the available experimental data for recombining plasmas shows that (i) all reliable results in recombination-rate determinations are restricted to a range of electron temperatures and densities at which the critical collision rates occur at relatively small n; (ii) in the experimental results, as the critical n increases, the determination of electron temperature becomes progressively more uncertain; (iii) the interpretation of measured recombination rates, in terms of a rate coefficient $\alpha(T_e, n_e)$ that is to be compared with calculated values, is exceedingly sensitive to errors in experimentally determined T_e; and (iv) no self-consistent detailed comparison between observed and calculated excited-state population densities over a wide range of conditions (T_e and n_e) has been satisfactorily achieved.

The present work was undertaken in an effort to extend the range of plasma conditions for which meaningful comparisons may be made between calculations and measurements. The goal of the endeavor is to deduce a semiempirical formula for the cross sections of collisional transitions between the excited states of helium that will reproduce the experimental observations and allow quantitative comparison with various theoretical predictions.

II. MEASUREMENTS

The present measurements were made in essentially the same way as those reported previously.[5,8,15] An Ohmic heating plasma was produced in the C stellarator,[16] with an electron density $n_e \sim 4\times10^{13}$ cm^{-3} and an electron temperature $T_e \sim 20$ eV, and the heating current was then terminated as rapidly as possible. The electron density was measured with microwave interferometers, and absolute intensities of most of the observable spectral lines were recorded as functions of time with calibrated monochromators. Then, assuming the plasma to be uniform along the line of sight,[17] and using well-known transition probabilities,[18] population densities of excited states of neutral and singly ionized helium were deduced.

For the conditions considered, electron temperatures ranged from 0.04 to 1 eV, electron densities from 10^{11} to 3×10^{13} cm^{-3}, and neutral helium densities from 5×10^{12} to 5×10^{13} cm^{-3}. This represents an extension by about an order of magnitude of the range of electron density for which reasonably reliable density and light-intensity measurements for stellarator afterglows are available.

In view of the similarity, in many respects, of measurements for several stellarator runs, we shall limit our discussion to two sets of observations, the results of which are presented in Figs. 1 – 4 and in Tables I and II. Since the only essential difference between the operating conditions for the two cases is the initial helium pressure, the results will serve to illustrate the reproducibility of certain aspects of the dependence of the measured population densities on electron density and temperature, and will show the effect of entrapment of resonance radiation.

Figures 1 and 2 show the average electron densities for the two cases as functions of time. The origins of the time axes are arbitrary but correspond roughly to the times at which the respective Ohmic heating currents were terminated. In each case the electron densities were determined from phase shifts of 4.3- and 8.6-mm microwave interferometers, assuming a path length equal to the nominal plasma diameter of 12.2 cm. The estimated accuracy of the electron-density measurements is ±15% in the early part of the afterglow, and ±30% late in the afterglow. Since n_e enters linearly in collisional transition rates, this sets a corresponding limit on the accuracy of the results discussed below.

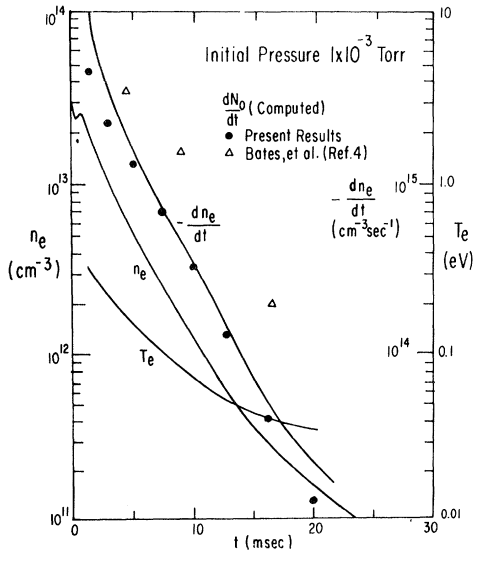

FIG. 1. Electron density n_e, temperature T_e, and loss rate $-dn_e/dt$ for a helium afterglow with initial neutral gas pressure of 1×10^{-3} Torr. Computed recombination rates are represented by solid circles (present results) and triangles (classical cross sections).

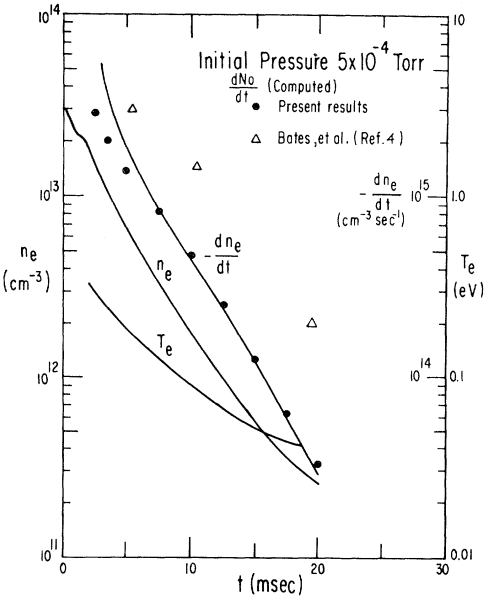

FIG. 2. Electron density n_e, temperature T_e, and loss rate $-dn_e/dt$ for a helium afterglow with initial neutral gas pressure of 5×10^{-4} Torr. Computed recombination rates are represented by solid circles (present results) and triangles (classical cross sections).

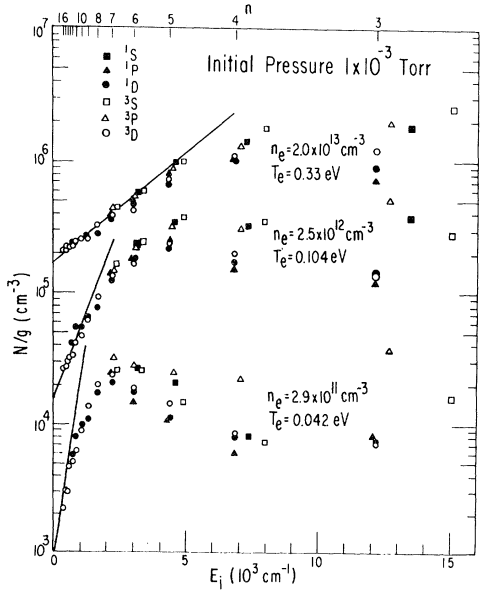

FIG. 3. Measured population densities of excited states of neutral helium for three different times in the afterglow of Fig. 1.

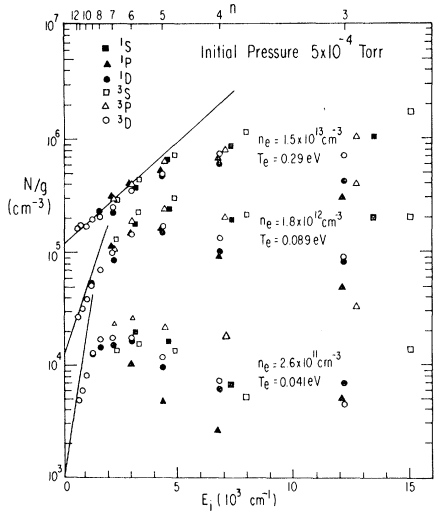

FIG. 4. Measured population densities of excited states of neutral helium for three different times in the afterglow of Fig. 2.

The slight difference in decay times of the electron densities of Figs. 1 and 2 results from the difference in initial gas pressure and reflects a more rapid cooling of the plasma for the higher-pressure case.

The determination of electron temperature, which is of crucial importance in comparisons of computed recombination-rate coefficients with measurements, and the remaining curves and points appearing in Figs. 1 and 2 will be discussed later.

Measured excited-state population densities N/g, where g is statistical weight, for typical plasma conditions are shown in Figs. 3 and 4, plotted against ionization potential E_i. The solid line for each set of points represents the Saha equilibrium population densities corresponding to the values of n_e and T_e as shown, assuming plasma neutrality $N_+ = n_e$. Observations of the He II spectrum indicated a negligible degree of second ionization for these measurements.

III. METHOD OF ANALYSIS OF MEASUREMENTS

For each plasma condition in Figs. 3 and 4, a critical value n_c of the principal quantum number n (approximately that for which the measured population densities are maximum) exists such that collisional and radiative transition rates to neighboring excited levels are equal. For $n > n_c$, collisional transitions are more important, and for $n < n_c$, radiative transitions dominate. The population densities of excited levels for $n < n_c$ relative to those for $n > n_c$ are largely determined by the collisional transition rates for levels with $n \sim n_c$ (and by the radiative transition rates). Therefore, a cross-section formula for which computed population densities are in good agreement with measurements should yield reasonably accurate transition-rate coefficients for levels in the neighborhood of n_c, provided that n_e and T_e are accurately known.

An analysis similar to the present one was reported earlier,[15] but because of the restricted range of plasma conditions and uncertainties in electron temperatures the results were inconclusive.

The method of calculating excited-state population densities for the helium plasmas under consideration is essentially the same as that used by Bates, Kingston, and McWhirter.[4] A transition-rate equation is written, for each of the atomic levels chosen to be distinct, in terms of collisional and radiative transitions to and from other discrete levels and the continuum. The time-derivative term in each equation, except that for the ground level, is assumed to be negligible compared to the other terms. Then, by invoking the conservation of atoms, there results a set of $k+1$ simultaneous, linear algebraic equations which can be solved for the population densities of k discrete levels and the rate of change of population density of the ground level.

The grouping of states into discrete levels and the treatment of ionization and radiative recombination for the present calculations are the same as described in Ref. 15. Rate coefficients for electron-induced bound-bound transitions differ from those of Ref. 15, however, as described in Sec. IV.

IV. CROSS SECTIONS

A suitable set of cross sections for describing excitation in a helium plasma must not only account for the relative population densities of states with different principal quantum numbers, but also for states with the same principal quantum number and different angular momenta or multiplicity. Certain features of the relative population densities of measurements such as those of Figs. 3 and 4 may be explained qualitatively in terms of optically allowed transitions within an LS coupling scheme. For example, one would expect the resonance transition to rapidly depopulate the ^1P states unless entrapment of the resonance radiation becomes important. This effect is apparently illustrated in the low-density measurements of Figs. 3 and 4, where the 3^1P state for both initial gas pressures – and the higher ^1P states for the higher pressure – show evidence of entrapment.[19] Conversely, the small radiative-transition probabilities for depopulating the ^3P states can be expected to result in an overpopulation of the ^3P series.

Some features of the measurements, however,

TABLE I. Population densities N/g (cm^{-3}) of excited states of neutral helium. Initial pressure = 1×10^{-3} Torr. (Superscripts in the table denote powers of 10 by which the numbers are to be multiplied.)

Time (msec)	0.50	0.75	1.0	1.3	3.0	5.1	7.5	10.0	12.7	16.2	20.0
n_e (cm^{-3})	2.4^{13}	2.5^{13}	2.4^{13}	2.0^{13}	1.0^{13}	5.0^{12}	2.5^{12}	1.25^{12}	6.1^{11}	2.9^{11}	1.61^{11}
T_e (eV)	1.1	0.65	0.42	0.33	0.23	0.151	0.104	0.074	0.052	0.042	0.036
State											
3^1S	•••	•••	1.5^6	1.80^6	9.9^5	6.3^5	3.7^5	1.72^5	•••	•••	•••
3^1P	5.7^4	2.4^5	6.6^5	7.3^5	3.7^5	2.1^5	1.22^5	6.1^4	2.6^4	8.4^3	2.5^3
3^1D	7.5^4	2.7^5	8.2^5	9.1^5	4.6^5	2.7^5	1.40^5	6.6^4	2.5^4	7.6^3	2.1^3
3^3S	2.6^5	7.6^5	2.2^6	2.5^6	1.10^6	5.9^5	2.9^5	1.25^5	4.9^4	1.59^4	•••
3^3P	2.1^5	7.2^5	1.90^6	1.96^6	1.20^6	8.7^5	6.1^5	3.4^5	1.46^5	4.7^4	1.50^4
3^3D	1.50^5	4.8^5	1.20^6	1.23^6	5.6^5	2.9^5	1.38^5	6.1^4	2.3^4	7.2^3	2.8^3
4^1S	9.8^4	4.1^5	1.24^6	1.42^6	8.9^5	5.8^5	3.2^5	1.36^5	4.2^4	8.1^3	•••
4^1P	7.9^4	2.5^5	7.5^5	1.06^6	5.9^5	3.4^5	1.55^5	6.5^4	2.3^4	6.0^3	1.80^3
4^1D	8.6^4	3.4^5	9.4^5	1.03^6	5.6^5	3.4^5	1.74^5	7.4^4	2.8^4	8.3^3	3.8^3
4^3S	1.35^5	5.3^5	1.55^6	1.82^6	1.11^6	7.0^5	3.4^5	1.31^5	3.6^4	7.4^3	•••
4^3P	9.0^4	3.9^5	1.10^6	1.30^6	8.0^5	5.2^5	3.1^5	1.61^5	7.3^4	2.3^4	6.9^3
4^3D	9.8^4	3.8^5	1.02^6	1.12^6	6.5^5	3.9^5	2.0^5	9.0^4	3.3^4	8.5^3	2.4^3
5^1S	7.9^4	2.9^5	7.9^5	1.00^6	6.8^5	5.1^5	3.5^5	1.90^5	8.3^4	2.1^4	5.0^3
5^1P	7.8^4	3.0^5	7.0^5	8.4^5	5.6^5	4.1^5	2.6^5	1.23^5	4.3^4	1.10^4	3.4^3
5^1D	6.7^4	2.2^5	6.0^5	7.0^5	4.7^5	3.6^5	2.2^5	1.10^5	4.3^4	1.15^4	4.2^3
5^3S	7.7^4	2.8^5	7.5^5	9.9^5	7.2^5	5.6^5	3.7^5	1.89^5	7.0^4	1.45^4	3.5^3
5^3P	7.5^4	2.6^5	6.8^5	9.0^5	6.2^5	4.7^5	3.2^5	1.77^5	7.9^4	2.4^4	7.4^3
5^3D	6.9^4	2.4^5	6.1^5	7.3^5	4.9^5	3.6^5	2.4^5	1.22^5	4.9^4	1.42^4	5.3^3
6^1S	6.2^4	1.60^5	4.0^5	5.8^5	3.8^5	3.0^5	2.3^5	1.52^5	7.8^4	2.7^4	8.6^3
6^1P	6.5^4	1.8^5	4.4^5	5.4^5	3.4^5	2.6^5	1.85^5	1.07^5	4.8^4	1.46^4	4.6^3
6^1D	4.8^4	1.33^5	3.2^5	4.9^5	3.3^5	2.5^5	1.84^5	1.19^5	5.9^4	1.81^4	6.2^3
6^3S	5.5^4	1.85^5	4.6^5	5.9^5	4.1^5	3.2^5	2.4^5	1.67^5	8.4^4	2.6^4	8.7^3
6^3P	5.1^4	1.67^5	4.2^5	5.6^5	3.8^5	3.0^5	2.3^5	1.52^5	8.2^4	2.8^4	9.4^3
6^3D	5.0^4	1.55^5	3.6^5	4.2^5	2.9^5	2.2^5	1.63^5	1.08^5	5.5^4	1.90^4	5.8^3
7^1P	•••	1.53^5	3.2^5	4.0^5	2.5^5	1.85^5	1.40^5	9.6^4	5.7^4	2.5^4	1.00^4
7^1D	4.5^4	1.30^5	3.0^5	3.6^5	2.3^5	1.69^5	1.25^5	8.4^4	5.0^4	2.1^4	8.2^3
7^3S	6.2^4	1.85^5	3.9^5	4.5^5	2.8^5	2.1^5	1.68^5	1.17^5	6.8^4	2.6^4	9.4^3
7^3P	5.1^4	1.75^5	3.7^5	4.4^5	2.8^5	2.1^5	1.52^5	1.09^5	7.1^4	3.3^4	1.31^4
7^3D	5.3^4	1.75^5	3.6^5	3.9^5	2.5^5	1.86^5	1.37^5	9.4^4	5.6^4	2.4^4	9.6^3
8^1D	4.4^4	1.16^5	2.6^5	2.8^5	1.66^5	1.14^5	7.8^4	5.4^4	3.3^4	1.76^4	8.6^3
8^3D	5.2^4	1.50^5	3.1^5	3.3^5	1.92^5	1.32^5	9.3^4	6.3^4	4.1^4	2.0^4	8.6^3
9^1D	4.8^4	1.08^5	2.1^5	2.6^5	1.53^5	1.02^5	6.6^4	4.1^4	2.4^4	1.10^4	5.0^3
9^3D	4.5^4	1.35^5	2.5^5	2.6^5	1.47^5	9.6^4	6.3^4	4.1^4	2.6^4	1.38^4	6.3^3
10^1D	5.3^4	1.20^5	2.4^5	2.5^5	1.39^5	8.7^4	5.6^4	3.5^4	2.1^4	1.02^4	5.1^3
10^3D	4.5^4	1.07^5	2.3^5	2.5^5	1.27^5	7.9^4	4.8^4	2.9^4	1.74^4	9.0^3	4.9^3
11^1D	•••	1.30^5	2.3^5	2.4^5	1.38^5	8.8^4	5.5^4	3.1^4	1.70^4	8.1^3	3.7^3
11^3D	4.4^4	1.10^5	2.3^5	2.5^5	1.22^5	7.2^4	4.2^4	2.5^4	1.41^4	6.7^3	3.3^3
12^1D	•••	1.47^5	2.8^5	2.5^5	1.19^5	7.2^4	4.1^4	2.3^4	1.21^4	5.8^3	2.8^3
12^3D	4.1^4	1.04^5	2.0^5	2.2^5	1.11^5	6.1^4	3.4^4	1.89^4	1.04^4	5.2^3	2.5^3
13^3D	4.2^4	9.6^4	1.85^5	2.2^5	1.07^5	5.8^4	3.3^4	1.88^4	1.02^4	4.8^3	2.3^3
14^3D	•••	9.8^4	1.85^5	2.2^5	1.05^5	5.6^4	3.0^4	1.47^4	7.0^3	3.0^3	1.30^3
15^3D	4.6^4	1.04^5	1.70^5	2.1^5	1.02^5	5.2^4	2.8^4	1.43^4	7.3^3	3.1^3	1.33^3
16^3D	•••	7.7^4	1.60^5	2.1^5	9.7^4	5.2^4	2.8^4	1.30^4	5.5^3	2.2^3	8.9^2

cannot be accounted for by optically allowed transitions alone. For example, calculations such as those of Ref. 15, which do not include optically forbidden transitions among the excited LS coupled states, often exhibit a separation between n^1D and n^3D population densities because of the rapid depopulation of the ^1P states via the resonance transitions. But, as may be seen from Figs. 3 and 4, this is not observed in any of the present measurements for $n > 3$. The precise cause for this similarity of ^1D and ^3D population densities is uncertain, although observations for a range of initial

TABLE II. Population densities N/g (cm^{-3}) of excited states of neutral helium. Initial pressure $= 5 \times 10^{-4}$ Torr. (Superscripts in the table denote powers of 10 by which the numbers are to be multiplied.)

Time (msec)	1.2	1.5	2.0	2.5	3.5	5.0	7.5	10.0	12.5	15.0	17.5	20.0
n_e (cm^{-3})	2.1^{13}	2.0^{13}	1.79^{13}	1.5^{13}	1.01^{13}	6.4^{12}	3.3^{12}	1.80^{12}	9.9^{11}	5.8^{11}	3.6^{11}	2.6^{11}
T_e (eV)	0.85	0.52	0.33	0.29	0.24	0.183	0.125	0.089	0.066	0.052	0.044	0.041
State												
2^3P	1.40^7	3.3^7	5.4^7	3.7^7	2.0^7	1.14^7	6.4^6	3.6^6	1.9^6	1.01^6	5.3^5	2.9^5
3^1S	•••	3.9^5	1.12^6	1.00^6	7.3^5	5.4^5	3.4^5	1.97^5	•••	•••	•••	•••
3^1P	5.8^4	1.72^5	3.8^5	2.9^5	2.0^5	1.40^5	8.4^4	4.8^4	2.6^4	1.38^4	7.8^3	5.0^3
3^1D	7.6^4	2.0^5	4.9^5	4.2^5	3.0^5	7.6^4	1.38^5	8.0^4	4.2^4	2.3^4	1.22^4	6.8^3
3^3S	2.4^5	6.8^5	1.94^6	1.66^6	1.08^6	7.1^5	3.7^5	1.98^5	1.03^5	5.1^4	2.6^4	1.32^4
3^3P	1.74^5	4.6^5	1.19^6	9.9^5	7.9^5	6.5^5	5.1^5	3.8^5	2.3^5	1.22^5	6.3^4	3.3^4
3^3D	1.43^5	4.0^5	8.7^5	6.9^5	4.6^5	2.9^5	1.70^5	9.0^4	4.4^4	2.1^4	1.02^4	4.5^3
4^1S	1.50^5	4.0^5	9.6^5	8.5^5	6.5^5	5.0^5	3.4^5	1.88^5	9.5^4	4.1^4	1.75^4	6.6^3
4^1P	1.10^5	3.1^5	7.8^5	6.7^5	4.8^5	3.3^5	1.88^5	9.2^4	4.2^4	1.61^4	5.8^3	2.5^3
4^1D	9.5^4	2.6^5	6.5^5	5.9^5	4.3^5	3.1^5	1.83^5	1.00^5	5.0^4	2.4^4	1.19^4	6.0^3
4^3S	1.38^5	3.9^5	1.07^6	1.10^6	8.5^5	6.5^5	4.1^5	2.1^5	9.5^4	3.7^4	1.41^4	5.3^3
4^3P	1.10^5	3.2^5	8.4^5	7.8^5	6.0^5	4.6^5	3.2^5	2.0^5	1.15^5	6.5^4	3.6^4	1.90^4
4^3D	1.04^5	3.1^5	7.9^5	7.2^5	5.6^5	4.0^5	2.5^5	1.30^5	6.4^4	3.1^4	1.52^4	7.2^3
5^1S	8.6^4	2.6^5	6.4^5	6.4^5	5.1^5	4.2^5	3.3^5	2.4^5	1.36^5	6.7^4	3.1^4	1.58^4
5^1P	8.7^4	2.1^5	5.6^5	5.2^5	4.4^5	3.5^5	2.6^5	1.63^5	7.8^4	3.0^4	1.13^4	•••
5^1D	8.3^4	2.0^5	5.0^5	4.7^5	3.9^5	3.2^5	2.3^5	1.51^5	8.3^4	4.0^4	1.91^4	9.6^3
5^3S	1.03^5	2.7^5	7.4^5	7.1^5	6.0^5	5.1^5	4.3^5	3.0^5	1.59^5	7.8^4	3.2^4	1.31^4
5^3P	8.8^4	2.4^5	6.5^5	6.3^5	5.1^5	4.3^5	3.3^5	2.4^5	1.42^5	7.5^4	4.0^4	2.1^4
5^3D	8.4^4	2.2^5	5.3^5	4.9^5	4.0^5	3.3^5	2.5^5	1.70^5	9.4^4	5.0^4	2.4^4	1.15^4
6^1S	7.3^4	1.63^5	3.9^5	3.7^5	3.1^5	2.7^5	2.3^5	1.78^5	1.27^5	7.7^4	4.0^4	1.90^4
6^1P	1.08^5	2.3^5	4.3^5	4.0^5	3.2^5	2.6^5	2.0^5	1.50^5	9.6^4	5.1^4	2.4^4	1.00^4
6^1D	6.7^4	1.70^5	3.9^5	3.5^5	2.8^5	2.4^5	1.93^5	1.45^5	9.4^4	5.4^4	2.9^4	1.63^4
6^3S	7.4^4	1.88^5	4.5^5	4.4^5	3.6^5	3.1^5	2.8^5	2.3^5	1.55^5	9.2^4	4.7^4	2.5^4
6^3P	7.5^4	1.75^5	4.3^5	4.0^5	3.1^5	2.7^5	2.2^5	1.78^5	1.23^5	7.8^4	4.5^4	2.6^4
6^3D	8.0^4	1.80^5	3.8^5	3.5^5	2.9^5	2.4^5	1.90^5	1.47^5	1.00^5	5.7^4	3.2^4	1.75^4
7^1P	9.7^4	1.87^5	3.4^5	3.1^5	2.4^5	1.88^5	1.48^5	1.11^5	7.8^4	5.1^4	3.1^4	1.62^4
7^1D	6.1^4	1.33^5	2.5^5	2.2^5	1.82^5	1.48^5	1.15^5	8.6^4	6.1^4	4.2^4	2.7^4	1.50^4
7^3S	6.6^4	1.54^5	3.1^5	2.9^5	2.3^5	1.88^5	1.54^5	1.28^5	9.8^4	6.6^4	4.0^4	2.4^4
7^3P	7.5^4	1.40^5	3.3^5	3.0^5	2.1^5	1.67^5	1.30^5	1.03^5	8.0^4	5.6^4	3.6^4	2.3^4
7^3D	6.0^4	1.30^5	2.8^5	2.5^5	1.93^5	1.60^5	1.27^5	1.00^5	7.2^4	4.7^4	3.0^4	1.75^4
8^1D	4.7^4	1.05^5	2.5^5	2.3^5	1.63^5	1.26^5	9.3^4	7.1^4	5.3^4	3.7^4	2.4^4	1.45^4
8^3D	5.6^4	1.20^5	2.3^5	2.1^5	1.60^5	1.29^5	9.4^4	7.1^4	5.2^4	3.7^4	2.5^4	1.65^4
9^1D	5.5^4	1.03^5	2.2^5	1.95^5	1.42^5	1.05^5	7.5^4	5.5^4	3.8^4	2.6^4	1.78^4	1.26^4
9^3D	4.9^4	1.00^5	2.1^5	1.95^5	1.40^5	1.04^5	7.2^4	5.2^4	3.9^4	2.8^4	1.85^4	1.27^4
10^3D	4.7^4	1.00^5	1.88^5	1.72^5	1.18^5	8.7^4	5.7^4	3.9^4	2.6^4	1.80^4	1.20^4	8.0^3
11^3D	4.8^4	9.5^4	1.95^5	1.75^5	1.18^5	8.0^4	5.2^4	3.2^4	2.2^4	1.40^4	9.2^3	6.0^3
12^3D	3.9^4	7.6^4	1.72^5	1.65^5	1.09^5	7.1^4	4.4^4	2.7^4	1.70^4	1.08^4	7.2^3	4.8^3

gas pressures show that imprisonment of resonance radiation cannot be responsible. It may reflect a partial breakdown of LS coupling for the higher nL states, as has been suggested by several authors in connection with excitation-transfer phenomena.[12] In the present calculations we merely assume that there are direct electron-induced collisional transitions between singlet and triplet states with the same principal quantum number and orbital angular momentum for $L > 2$. In this case the rate coefficients required are at least 5% of those for the corresponding $n^1P \rightarrow n^1D$ transitions.

We have taken, for the cross section for dipole transitions from a lower level p to an upper level q, the expression

$$\sigma_{pq}(U_{pq}) = 4\left(\frac{E_H}{E_{pq}}\right)^2 f_{pq}\pi a_0^2 F_{pq}(U_{pq}), \qquad (1)$$

where E_{pq} is the transition energy, f_{pq} is the absorption oscillation strength, U_{pq} is the normalized impact energy,

$$U_{pq} = E/E_{pq} \geq 1, \qquad (2)$$

and a_0 and E_H are the Bohr radius and the rydberg (13.6 eV), respectively. $F_{pq}(U_{pq})$ was assumed to be of the form

$$F_{pq}(U_{pq}) = U_{pq}^{-1}(1 - e^{-r_{pq}(U_{pq}+1)})\ln(U_{pq} + \delta), \qquad (3)$$

where $$r_{pq} = \beta(f_{pq}E_H/E_{pq})^{-\gamma}, \qquad (4)$$

and β, γ, and δ are non-negative, dimensionless, adjustable parameters, independent of p and q.

For large impact energies ($U_{pq} \rightarrow \infty$), $F_{pq}(U_{pq})$ has the asymptotic form

$$F_{pq} \sim U_{pq}^{-1} \ln U_{pq}, \qquad (5)$$

so that Eq. (1) reduces to the Bethe approximation. At small U_{pq}, the shape and size of the cross sections are determined by the three parameters: a change of β varies the magnitudes of all the cross sections; a change in γ produces a systematic variation of the cross sections with line strength, relative to the variation produced by β; and a finite δ allows the cross sections to remain finite at $U_{pq} = 1$.[20]

The Gryziński classical cross sections for $n \rightarrow n+1$ transitions in hydrogen are adequately represented by the choice $\beta = 1$, $\gamma = 0.4$, $\delta = 0$. A choice of $\beta = 1.2$, $\gamma = 0.7$, $\delta = 0$ reproduces satisfactorily the impact-parameter cross sections.[14,21]

In Ref. 15, Eq. (3) with $r_{pq} = E_{pq}/(3.4\text{ eV})$ and $\delta = 0$ was used to represent the impact-parameter approximation cross sections. Although this choice gives an adequate representation for the total $n \rightarrow n+1$ transitions, it leads to an underestimate of the cross sections of relatively small dipole strength (e.g., $n \rightarrow n+2$), and thus contributes to the discrepancies between measured and computed population densities noted in Ref. 15. In addition to this change in the scaling in Eq. (3), it appears that optically forbidden transitions should be explicitly included in the calculation. In Ref. 15, optically forbidden transitions were ignored with the assumption that their effect would be indistinguishable, in comparison with experiment, from a minor modification of the cross sections for allowed transitions. However, this is not always true, especially in the case of the ^1S states. If the forbidden transitions were negligible, the n^1S states would show much stronger coupling to the n^1P states than is actually observed.

We have, therefore, explicitly introduced cross sections for optically forbidden ($\Delta L \neq 1$) transitions into some of our present calculations, in order to investigate the extent of the resulting improvement in agreement between calculated and measured population densities. In analogy with Eqs. (1)–(5), the cross sections used for this purpose are

$$\sigma_{pq}^{f}(U_{pq}) = 4(E_H/E_{pq})B_{pq}\pi a_0^2 F_{pq}^{f}(U_{pq}), \qquad (6)$$

where $$F_{pq}^{f}(U_{pq}) = U_{pq}^{-2}(1 - e^{-r_{pq}^{f}U_{pq}}) \times (U_{pq} - 1 + \delta)_{U_{pq}\infty} U_{pq}^{-1}, \qquad (7)$$

and $$r_{pq}^{f} = 1.6\,\beta B_{pq}^{-\gamma}\left[\left(\frac{R_0}{a_0}\right)^2 \frac{E_{pq}}{4E_H}\right]^{1-\gamma}, \qquad (8)$$

with β, γ, and δ the same parameters as in Eqs. (3) and (4). If one inserts asymptotic value of F_{pq}^{f} as given in (7), then the cross section (6) reduces to the Born approximation, and for B_{pq} we have used values interpolated from the hydrogenic cross sections of Kingston and Lauer.[22] (B_{pq} is one-half their tabulated $B_{n,l;\,n',l'}$.) The quantity R_0 in Eq. (8) is the lower cutoff value[18,23] for the impact parameter, which we have taken to be

$$R_0 = a_0 n_p^* n_q^*, \qquad (9)$$

where n_p^* and n_q^* are the effective quantum numbers for levels p and q.

If the impact parameter results of Stauffer and McDowell[23] are restricted such that the transition probability with impact parameter $R > R_0$ may not exceed $\frac{1}{2}$ (corresponding to Seaton's strong coupling case[14]), then the resulting cross sections for

quadrupole transitions at low impact energies may be satisfactorily represented by Eqs. (6)–(8) with $\beta = 1.2$, $\gamma = 0.7$, and $\delta = 0$, i.e., the same choice for which Eqs. (1)–(4) adequately represent impact-parameter cross sections for strong dipole transitions. With different choices of the parameters β, γ, δ, the near-threshold behavior of the cross sections for forbidden transitions may be varied in qualitatively the same fashion as for allowed transitions.

The populations of the excited states of helium are now computed, as described in the preceding section, using cross sections given in Eqs. (1)–(8) for the transition rates. The set of parameters β, γ, δ are varied to optimize the agreement with the experimental values over the observed range of the plasma conditions. The results and the effects of variation of some of the parameters are described in Sec. V.

V. RESULTS

Examples of calculated population densities for the plasma conditions of Fig. 4 are shown in Fig. 5. The plotted points are ratios of computed population densities to measured values, averaged for each principal quantum number n using the statistical weight as the weighting factor.

For the points in Fig. 5(a) forbidden transitions were explicitly included as discussed above, and β was changed by factors of 2 from one set of points to the next with $\gamma = 0.7$ and $\delta = 0$. For $n \rightarrow n+1$ transitions this corresponds roughly to changing all cross sections at low and intermediate energies by factors of 2. The approximate position of n_c is indicated by an arrow for each plasma condition.

For the points in Fig. 5(b) the parameter γ was varied, with β adjusted to keep the cross section for the $6 \rightarrow 7$ transition constant, and with $\delta = 0$. Nonexchange forbidden transitions among excited levels were not explicitly included, but cross sections for dipole transitions were increased with respect to the calculations of Fig. 5(a) ($\beta = 1.5$ versus $\beta = 0.6$, for $\gamma = 0.7$) in order to maintain agreement with measurements. The effect of this latter change on the averaged population densities is minute, as may be seen by comparing the solid dots in Figs. 5(a) and 5(b).

Results of calculations assuming cross sections with finite threshold values ($\delta = 0.2$) are shown in Fig. 5(c), again including forbidden transitions as in Fig. 5(a). Cross sections were held fixed while the electron temperature was changed from one set of points to the next by about 20%.

Figure 5 illustrates a number of important features of the calculated population densities. A change in the assumed cross sections has a pronounced effect on the population densities of levels with $n \lesssim n_c$ but almost no effect on levels with $n > n_c$. The cross sections that connect levels in the neighborhood of n_c, where collisional transition rates are comparable with radiative rates, are largely responsible for determining relative population densities. At $n \ll n_c$ or $n \gg n_c$, the cross sections may vary considerably without much effect on populations.

A modest change in the assumed temperature, with cross sections held fixed, results in a substantial change in the computed absolute population densities, but little change in relative population densities. We have, therefore, concentrated upon comparisons of computed and measured relative population densities, adjusting the electron temperature to bring absolute population densities into agreement for $n \gtrsim 10$. The electron tempera-

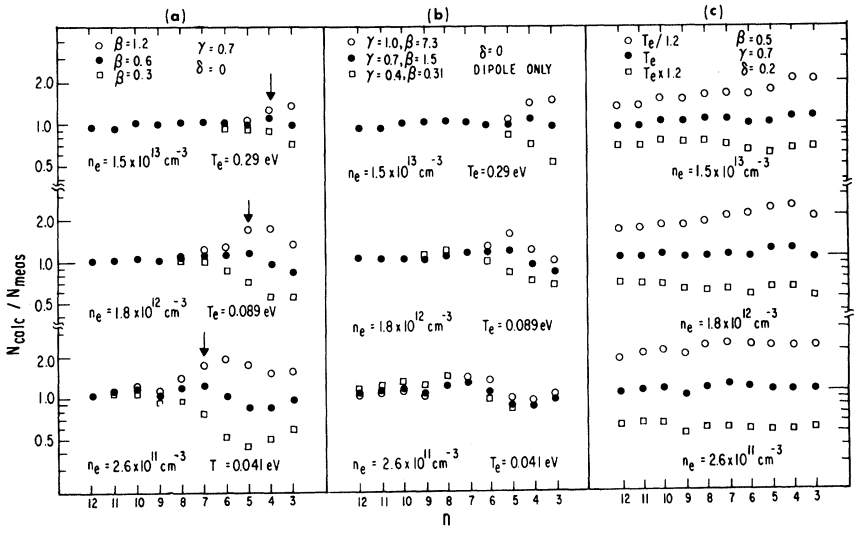

FIG. 5. Ratios of computed population densities to measured values of Fig. 4 for different assumed cross-section formulas (a) and (b), and for different assumed electron temperatures (c). Points are weighted averages for each value of the principal quantum number n. The approximate position of n_c is indicated for each condition by an arrow.

tures obtained in this way are insensitive to the assumed cross sections, varying by no more than 0.002 eV for any of the cross-section formulas considered; and small errors in T_e, introduced by errors in measurement of n_e or intensities, have little effect on conclusions based upon relative population densities.

For the range of plasma conditions shown, where $3 \lesssim n_c \lesssim 8$, the measured population densities may be reproduced to within about 20%, using $\gamma = 0.7$ in Eqs. (4) and (8). In this range, the quantity $f_{pq}E_H/E_{pq}$, for an $n \to n+1$ transition with $n \sim n_c$, changes by more than an order of magnitude. The calculations represented in Fig. 5(b) indicate that in order to obtain satisfactory agreement between computed and measured population densities throughout this range of n_c using Eqs. (3), (4), (7), and (8), we must have $\gamma = 0.7 \pm 0.3$. With given γ, the value of β can be determined to about ±30%, according to Fig. 5(a).

The agreement between computed and measured population densities appears to be somewhat better for $\delta = 0.2$ (finite threshold values) than for $\delta = 0$ (zero threshold values), although the differences are small. In either case, the cross section required for a strong dipole transition (when forbidden transitions are also included in the calculations) is approximately half that predicted by the impact-parameter approximation. If nonexchange forbidden transitions are not explicitly included in the calculations, the cross sections that one must assume for the allowed transitions in order to

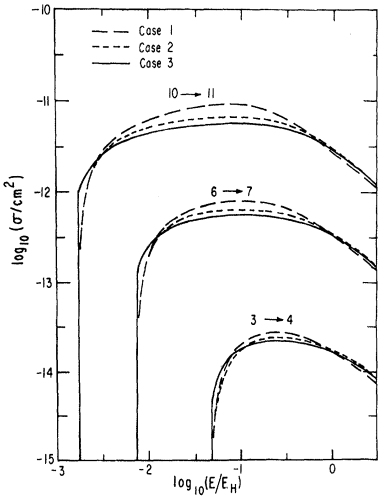

FIG. 6. Cross sections for $n \to n+1$ transitions using cross-section formulas optimized under three sets of assumptions: case (1), allowed transitions only with zero threshold values; case (2), allowed and forbidden transitions with zero threshold values; case (3), allowed and forbidden transitions with finite threshold values.

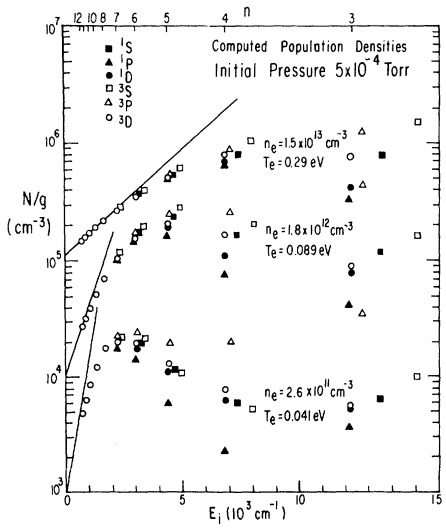

FIG. 7. Computed population densities of excited states of neutral helium using an optimized cross-section formula described in the text. The points are to be compared with the measurements of Fig. 4.

achieve the best agreement with measurements are somewhat larger than the impact-parameter results.

Figure 6 shows representative cross sections for $n \to n+1$ transitions for three cases, in each of which the parameter γ was taken to be 0.7 and β was adjusted to give best agreement with measured population densities: (i) zero threshold values ($\delta = 0$) and no nonexchange forbidden transitions (dashed curves); $\beta = 1.5$; (ii) zero threshold values with forbidden transitions included (dotted curves); $\beta = 0.6$; and (iii) finite threshold values ($\delta = 0.2$), with forbidden transitions included (solid curves); $\beta = 0.5$.

The cross sections are summed over final states and averaged over initial states in the plotted curves. Although the interpretation of each of the three cases in terms of specific transitions is different, the effective cross section for an $n \to n+1$ transition is essentially the same, especially for electron energies about twice the threshold energy. The agreement with the measured populations of the different levels with the same principal quantum number is best for case (iii), poorest for case (i), especially for the n^1S levels. Figure 7 shows the computed population densities for the plasma conditions of Fig. 4, using the cross sections of case (iii). Evidently, the essential features of the measurements are well represented.

In Fig. 8 the $n \to n+1$ cross sections for case (iii) are compared with impact-parameter approximation cross sections for hydrogen using dipole transitions only,[21] and with the classical cross sections used by Bates *et al.*[4] Clearly the present results

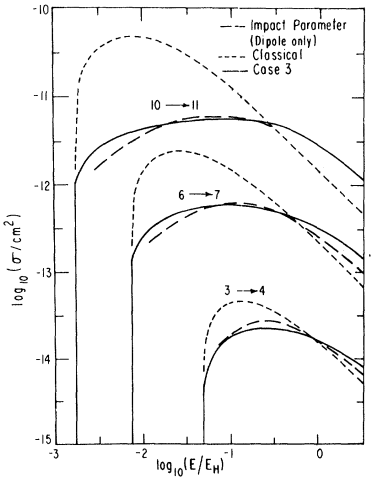

FIG. 8. Cross sections for $n \rightarrow n+1$ transitions, comparing the optimized formula for case (3) described in the text (solid curves) with results for hydrogen, using the classical approximation (dotted curves) and the impact-parameter approximation, neglecting forbidden transitions (dashed curves).

are in much closer accord with impact-parameter cross sections than with classical cross sections. If cross sections as large as the classical results are assumed in the present calculations, the discrepancy between computed and measured population densities for the lower levels is approximately equal to the ratio of the classical cross section for the $n_C \rightarrow n_C+1$ transition to the corresponding cross sections of Fig. 6 at intermediate electron energies.

As a further example of the inability of classical cross sections to account for our observations, computed recombination rates are plotted in Figs. 1 and 2 along with $-dn_e/dt$ obtained from the slope of the measured electron-density curves. The solid circles were computed using cross sections of Fig. 6. Except for minor discrepancies which may be attributed to spatial variations and plasma transport along the machine axis, the agreement between the solid circles and the $-dn_e/dt$ curves is good. On the other hand, the triangles, which represent recombination rates interpolated from the tables of Bates *et al.*,[4] clearly do not agree with the observed rates of electron loss, especially for low temperatures and densities. (When cross sections comparable to Gryziński's are assumed in the present calculations for helium, the results are essentially the same as those of Ref. 4.)

In previous work on recombination in helium afterglows,[5,8] a reasonable agreement has been reported with calculations based on classical cross sections. The discrepancy between those results and the present report is fairly modest at higher temperatures and densities, but becomes quite substantial at lower temperatures – especially at extrapolations beyond the range of measurements. The origin of the discrepancy lies in the determination of electron temperature in the recombining plasma. At low densities, the electron temperature in the old measurements was determined from plasma conductivity.[6] It now appears that these temperature measurements must be 20–30% too high (less so at higher densities). Some of the temperatures determined from the Saha equation in Ref. 5 are likewise too high, especially at lower densities and for $T_e \lesssim 0.15$ eV. Because of the very strong temperature dependence of the recombination-rate coefficient, such temperature differences have an appreciable effect on the recombination rates.

It must be emphasized that the present results are not based primarily on total recombination rates, but on detailed comparison of calculated and measured population densities of the excited states of helium over a large range of electron densities and temperatures. Since the measurement of the collisional transition rates is independent of such factors as possible axial variations of electron density and temperature in the stellarator (which somewhat affect the observed total recombination rates), and because of the increased range of the observed conditions, the reliability of the present results represents a considerable improvement over previous measurements.

The foregoing conclusions were based upon measurements at low temperatures. A further result may be deduced by considering the earlier part of the afterglow. When the electron temperature is in the range $0.3 \lesssim T_e \lesssim 1$ eV, the computed population densities of the lower excited states, especially the 2^3P level, are affected by the rate of depopulation of the 2^3S metastable level. The 1^1S-2^3S excitation cross section[12] cannot account for the required rate of depopulation of the 2^3S level. The only other transition fast enough to bring calculations and measurements for the 2^3P level into agreement is the $2^3S \rightarrow 2^1S$ transition. If we suppose that the cross section for the $2^3S \rightarrow 2^3P$ transition is represented with reasonable accuracy by one of the optimized cross-section formulas discussed above, and take

$$\sigma(2^3S \rightarrow 2^1S) = \sigma_0(U-1)/U^3 \qquad (10)$$

for the cross section for the $2^3S \rightarrow 2^1S$ transition, then in order to obtain good agreement between computed and measured population densities we must have $\sigma_0 = 70\pi a_0^2 \pm 50\%$.

VI. SUMMARY

By comparing measured excited-state population densities for helium afterglows with solutions of

transition rate equations we draw the following conclusions:

(a) For transitions not involving change of multiplicity, the cross sections given in Eqs. (1) and (6), with $\beta = 0.5$, $\gamma = 0.7$, and $\delta = 0.2$, reproduce the measured population densities adequately over the entire range of plasma conditions. These cross sections are in distinctly better accord with the results of the semiclassical impact-parameter approximation than with those of the classical impulse approximation.

(b) The transfer of excitation between ^1D and ^3D levels for the plasma conditions under consideration is rapid, and may not be attributed to imprisonment of resonance radiation or to transfer induced by neutral atoms. If the peak cross section for the $2^3S \rightarrow 2^1S$ transition is to reproduce the measured population densities for the 2^3P level in calculations, a value of $10\,\pi a_0^2$ (within about a factor of 2) is required.

ACKNOWLEDGMENTS

This work was performed under the auspices of the U. S. Atomic Energy Commission, Contract AT(30-1)-1238; use was also made of computer facilities supported in part by National Science Foundation Grant No. NSF-GP579.

[1]See, for example, C. Park, J. Quant. Spectr. Radiative Transfer 8, 1633 (1968); D. W. Norcross and P. M. Stone, *ibid.* 8, 655 (1968).

[2]M. Gryziński, Phys. Rev. 115, 374 (1959).

[3]M. Gryziński, Phys. Rev. 138, A336 (1965).

[4]D. R. Bates, A. E. Kingston, and R. W. P. McWhirter, Proc. Roy. Soc. (London) A267, 297 (1962); A270, 155 (1962).

[5]E. Hinnov and J. G. Hirschberg, Phys. Rev. 125, 795 (1962).

[6]R. W. Motley and A. F. Kuckes, Proceedings of the Fifth International Conference on Ionization Phenomena, Munich, 1961 (North-Holland Publishing Co., Amsterdam, 1962), p. 651.

[7]Yu. M. Aleskovskii and V. L. Granovskii, Zh. Eksperim. i Teor. Fiz. 43, 1523 (1962) [English transl.: Soviet Phys. – JETP 16, 887 (1963)].

[8]E. Hinnov, Phys. Rev. 147, 197 (1966).

[9]S. von Goeler, R. W. Motley, and R. Ellis, Phys. Rev. 172, 162 (1968).

[10]D. R. Bates and A. E. Kingston, Proc. Roy. Soc. (London) A279, 10 (1964); A279, 32 (1964).

[11]A. Burgess and I. C. Percival, in Advances in Atomic and Molecular Physics, edited by D. R. Bates and I. Estermann (Academic Press Inc., New York, 1968), Vol. 4.

[12]B. L. Moiseiwitsch and S. J. Smith, Rev. Mod. Phys. 40, 238 (1968).

[13]P. G. Burke, United Kingdom Atomic Energy Authority Report No. AERE-L 170, 1967 (unpublished).

[14]M. J. Seaton, Proc. Phys. Soc. (London) 79, 1105 (1962).

[15]L. C. Johnson, Phys. Rev. 155, 64 (1967); see also Princeton Plasma Physics Laboratory Report No. MATT-436, 1966 (unpublished).

[16]For a description of the C stellarator and Ohmic heating plasmas see R. M. Sinclair, S. Yoshikawa, W. L. Harries, K. M. Young, K. E. Weimer, and J. L. Johnson, Phys. Fluids 8, 118 (1965); A. S. Bishop, A. Gibson, E. Hinnov, and F. W. Hofmann, *ibid.*, 8, 1541 (1965); J. G. Hirschberg and E. Hinnov, J. Chem. Phys. 45, 2233 (1966).

[17]The replacement of the actual plasma by a homogeneous cylindrical model with a radius determined by the divertor field configuration results in errors that are small compared to the experimental uncertainties of the light-intensity and electron-density measurements. In the actual plasmas, T_e is known to be constant within the divertor aperture, and to drop rapidly outside. The density varies somewhat within the aperture with various conditions, but intensities obtained from calculated population densities, by assuming variations of observed order and numerically integrating along the line of sight, could not be clearly distinguished from those obtained using the uniform-cylinder model.

[18]W. L. Wiese, M. W. Smith, and B. M. Glennon, Atomic Transition Probabilities (National Bureau of Standards, Washington, D. C., 1966), Vol. I.

[19]Entrapment of resonance radiation in Ref. 15 was treated using a uniform sphere model and assuming Doppler-broadened lines. A more detailed study of the problem, including spatial variations along the line of sight, the Voigt line profile, and possible differences between ion and neutral temperatures, gives results which agree with those of the uniform sphere model to within the uncertainty introduced by possible errors in the measurements of the initial pressure.

[20]P. G. Burke, S. Ormonde, and W. Whitaker, Proc. Phys. Soc. (London) 92, 319 (1967).

[21]H. E. Saraph, Proc. Phys. Soc. (London) 83, 763 (1964).

[22]A. E. Kingston and J. E. Lauer, Proc. Phys. Soc. (London) 87, 399 (1966); 88, 597 (1966).

[23]A. D. Stauffer and M. R. C. McDowell, Proc. Phys. Soc. (London) 85, 61 (1965); 89, 289 (1966).